

# FTIR Spectroscopic Evidence for the Involvement of an Acidic Residue in Quinone Binding in Cytochrome *bd* from *Escherichia coli*<sup>†</sup>

Jie Zhang,<sup>‡</sup> Walter Oettmeier,<sup>§</sup> Robert B. Gennis,<sup>‡</sup> and Petra Hellwig<sup>\*,||</sup>

Department of Biochemistry, University of Illinois, 600 South Mathews Avenue, Urbana, Illinois 61801,  
Lehrstuhl für Biochemie der Pflanzen Universitätsstrasse 150, Universität Bochum, Bochum, Germany, and  
Institut für Biophysik, Universität Frankfurt, Theodor-Stern-Kai 7 Haus 75, 60590 Frankfurt, Germany

Received September 11, 2001; Revised Manuscript Received January 3, 2002

**ABSTRACT:** In this work, FTIR difference spectroscopy is used to search for possible binding partners and protonable groups involved in the binding of the quinol to cytochrome *bd* from *Escherichia coli*. In addition, the electrochemically induced FTIR difference spectra are compared for preparations of the enzyme isolated from cells grown at different oxygen levels in which the quinone content of the membrane is altered. On this basis, difference signals can be tentatively attributed to the vibrational modes of the different quinones types that are associated with the enzyme depending on growth conditions. Furthermore, vibrational modes due to the redox-dependent reorganization of the protein vary depending on the quinone associated with the isolated enzyme. Of particular interest are the observations that a mode at 1738 cm<sup>-1</sup> is decreased and a mode at 1595 cm<sup>-1</sup> is increased as observed in direct comparison to the data obtained from samples grown anaerobically. These signals indicate a change in the protonation state of an aspartic or glutamic acid. Since these changes are observed when the ubiquinone ratio in the preparation increases, the data provide evidence for the modulation of the binding site by the interacting quinone and the involvement of an acidic group in the binding site. The tentative assignments of the vibrational modes are supported by electrochemically induced FTIR difference spectra of cytochrome *bd* in the presence of the specific quinone binding site inhibitors heptylhydroxyquinoline-*N*-oxide (HQNO) or 2-methyl-3-undecylquinolone-4. Whereas HQNO leads to strong shifts in the FTIR redox difference spectrum, 2-methyl-3-undecylquinolone-4 induces a specific shift of a mode at 1635 cm<sup>-1</sup>, which likely originates from the displacement of the C=O group of the bound quinone.

Cytochrome *bd* is a widely distributed bacterial oxidase. In the respiratory chain of *Escherichia coli*, it is expressed under microaerophilic growth conditions (1–5). It contains three heme redox centers, one low-spin heme *b*<sub>558</sub>, one high-spin heme *b*<sub>595</sub>, and one high-spin heme *d*. Heme *b*<sub>558</sub> functions as the primary input site for quinols. Heme *b*<sub>595</sub> and heme *d* have been proposed to form a diheme center where oxygen is bound and reduced to water (6, 7). In a process coupled to the prior one, protons are taken up from the cytoplasm and released into the periplasm, leading to the generation of a proton motive force (8). A hydrophilic loop, between transmembrane helices VI and VII in subunit I (the “Q loop”), has been shown to be necessary for quinol oxidation, and probably comprises part of a quinol binding site (9–12). Furthermore, a semiquinone radical was found to be stabilized by cytochrome *bd* in the presence of excess decylubiquinone (13, 14). Several specific inhibitors for quinone binding sites are effective on cytochrome *bd* like,

for example, Aurachin D, which has been reported to act specifically on cytochrome *bd* and to induce a shift in the absorption of the low-spin heme *b*<sub>558</sub> component of the enzyme (15, 16). Miller et al. (39) previously reported a quinone-to-protein ratio of ~0.5 for purified cytochrome *bd*.

Depending on growing conditions, different quinone types are found in the membrane of *E. coli*. Whereas, under aerobic growing conditions, ubiquinone is predominant, demethylmenaquinone or menaquinone is observed at reduced oxygen levels (17, 18). Cytochrome *bd* can apparently use the different quinone types as substrates, despite the different structures and midpoint potentials, which vary over a range of 200 mV in solution (1). If the same site can bind to both ubiquinol and menaquinol, this site must be able to accommodate the structural and steric differences between the one- and two-ring quinone systems. Also, protein–quinol interactions have been shown to be essential for determining the midpoint potentials of protein-bound quinones, and this is doubtless crucial for the proper function of the enzyme. Modulation of the quinone midpoint potential may be induced by the orientation of the side chains in the protein site. For example, a difference in the redox potentials of up to ~70 mV between the two quinones bound to the bacterial reaction center is related to differences in methoxy group conformations (19). In addition, the varied interactions of incorporated quinones on protein residues within the binding

<sup>†</sup> Financial support is gratefully acknowledged from DFG Grant He-3150/1-1 to P.H. and a Grant HL16101 from the National Institutes of Health to R.B.G.

\* To whom correspondence should be addressed. E-mail: hellwig@biophysik.uni-frankfurt.de. Telephone: ++49-69-6301-4227. Fax: ++49-69-6301-5835.

<sup>‡</sup> University of Illinois.

<sup>§</sup> Universität Bochum.

<sup>||</sup> Universität Frankfurt.

pocket have also been demonstrated by EPR spectroscopy in recent work on the cytochrome *bo*<sub>3</sub> ubiquinol oxidase from *E. coli* (20).

Infrared spectroscopy is a sensitive method for studying the structural protonation changes in the protein that accompany the redox reaction of the quinones. The vibrational modes of the quinones in their different redox and protonation states can serve as reporter groups for steric and energetic factors such as hydrogen bonding, polar interactions, and distortion of the ring and substituents. This has been previously demonstrated for the vibrational modes of the quinones in the bacterial reaction center in light-induced FTIR<sup>1</sup> difference spectra (21, 22). The vibrational modes of quinones were also identified in the electrochemically induced FTIR difference spectra in the *bc*<sub>1</sub> complex (23) and in cytochrome *bo*<sub>3</sub> from *E. coli* (24). Assignments were supported by isotopically labeled quinones (21, 22, 24). Recently, photo-redox-induced FTIR difference spectra of cytochrome *bd* from *E. coli* were presented for the spectral range from 1800 to 1550 cm<sup>-1</sup>. The data, importantly, suggest the involvement of several protonated acidic groups in the reorganization of the protein concomitant with the change in the redox state of the enzyme (25). Observations from this work are confirmed and extended in the current work.

In this study, FTIR redox difference spectra are compared for wild-type cytochrome *bd* from *E. coli* grown at different oxygen levels, as well as for the enzyme bound to quinol binding site inhibitors HQNO and 2-methyl-3-undecylquinolone-4. Vibrational modes are identified that suggest protein conformational changes as well as protonation reactions that are concomitant with quinone binding or with the change in the redox state of the bound quinone.

## MATERIALS AND METHODS

**Sample Preparation.** Cells were obtained from the GO105/pTK1 strain, grown at the fermentation facility at the University of Illinois at 37 °C and pH 7 in a 200 L fermenter. Further purification was performed as reported previously by Zhang et al. (26). Quinone content was determined by HPLC analysis (data not shown). For studies with the inhibitors 2-methyl-3-undecylquinolone-4 (38) and HQNO, each was dissolved in ethanol and 1–3 μL of a saturated solution of the inhibitor was then added to 400 μL of diluted cytochrome *bd*. Samples were reconcentrated to 5–10 μL with Microcon centrifugation concentrators to a final concentration of approximately 0.4 mM. The inhibitors were present in a 10-fold excess in the final samples. Ubiquinone-3 and menaquinone-3 (vitamin K<sub>3</sub>) solutions were obtained by dispersing the quinone in the presence of dodecyl maltoside.

**Electrochemistry.** The ultra-thin layer spectroelectrochemical cell for UV–vis and IR detection and the potentiostat (Universitäts-Werkstatt, Freiburg, Germany) were gifts from W. Mäntle (University of Frankfurt, Frankfurt, Germany) and were used as previously described (27, 28). Sufficient transmission in the range from 1800 to 1000 cm<sup>-1</sup> was achieved with a path length of 6–8 μm. Experimental

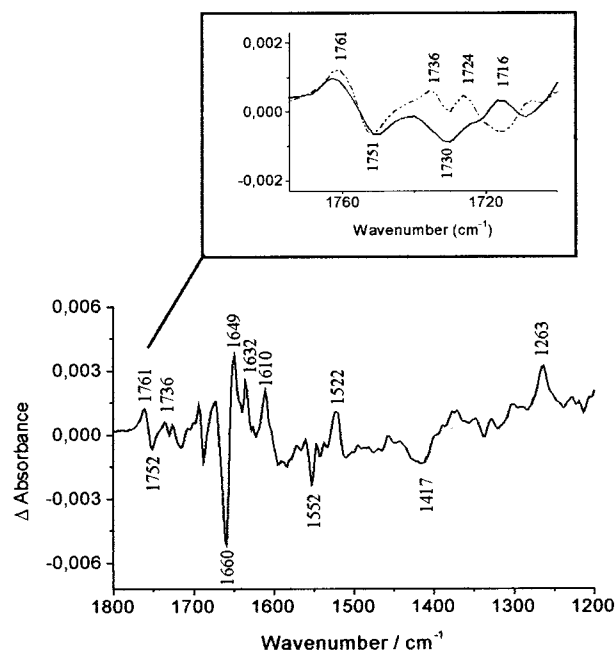


FIGURE 1: Oxidized-minus-reduced FTIR difference spectra of wild-type cytochrome *bd* from aerobically grown *E. coli* for a potential step from  $-0.5$  to  $0.5$  V (vs Ag/AgCl). The inset shows the enlarged view of the spectra from  $1770$  to  $1710$  cm<sup>-1</sup> for the sample equilibrated in H<sub>2</sub>O (—) and D<sub>2</sub>O (···).

conditions for cytochrome *bd* from *E. coli* were used as described previously (26, 29).

**FTIR Difference Spectroscopy.** FTIR difference spectra as a function of the applied potential were obtained in the range of 2500–1000 cm<sup>-1</sup> using a Bio-Rad model 575C instrument. In all experiments, the protein solution was first equilibrated at the initial potential of the electrode, and single-beam spectra in the IR range were recorded. Then, a potential step toward the final potential was applied, and the single-beam spectrum of this state was again recorded after equilibration. Subsequently, difference spectra, as presented in this work, were calculated from the two single-beam spectra with the initial single-beam spectrum taken as the reference. No smoothing or deconvolution procedures were applied. The equilibration at the applied potential generally took less than 5–6 min in the potential range from  $-0.5$  to  $0.5$  V. Equilibration times were determined by monitoring UV–vis difference spectra on the same sample (data not shown), and the full reaction in FTIR spectroscopy was monitored by double-difference spectra until no changes were detected. Typically, 320 interferograms at 4 cm<sup>-1</sup> resolution were co-added for each single-beam IR spectrum and Fourier transformed using triangular apodization. Five to ten difference spectra were usually averaged. The noise level in the difference spectra was estimated to be  $\sim 30$ – $50 \times 10^{-6}$  absorbance unit in the spectral range under consideration, except for the region of the strongly absorbing water bending and protein amide I modes at ca.  $1650$  cm<sup>-1</sup> where the noise was slightly higher.

## RESULTS AND DISCUSSION

**Electrochemically Induced FTIR Difference Spectra of Cytochrome *bd* from Aerobically Grown *E. coli*.** Figure 1 presents the oxidized-minus-reduced FTIR difference spectrum of cytochrome *bd* from *E. coli* for a potential step from

<sup>1</sup> Abbreviations: FTIR, Fourier transform infrared; SHE, standard hydrogen electrode; UQ, ubiquinone; MQ, menaquinone; HQNO, heptylhydroxyquinoline-*N*-oxide.

−0.5 to 0.5 V in the spectral range from 1800 to 1200  $\text{cm}^{-1}$ . The inset shows the enlarged view from 1770 to 1710  $\text{cm}^{-1}$  for the sample equilibrated in  $^1\text{H}_2\text{O}$  (full line) and  $^2\text{H}_2\text{O}$  buffer (dotted line). In the electrochemically induced FTIR difference spectra, contributions concomitant with electron transfer and coupled proton translocation can be expected from the reorganization of hemes *b* and *d*, of secondary structure elements, and of individual amino acids. In the amide I range (1690–1620  $\text{cm}^{-1}$ ), difference signals at 1672, 1660, and 1649  $\text{cm}^{-1}$  indicate absorbance changes of C=O modes caused by small alterations in the polypeptide backbone accompanying the redox process, as well as possible contributions from C=O modes of individual amino acid side chains (Asn and Gln). In the amide II range (1570–1520  $\text{cm}^{-1}$ ), coupled CN stretching and NH bending modes are expected. In addition, vibrational modes from aromatic amino acids and heme C=C modes from the porphyrin ring, for example, at 1572, 1552, and 1522  $\text{cm}^{-1}$ , are observable. Antisymmetric  $\text{COO}^-$  modes from deprotonated heme propionates and Asp or Glu side chains, caused by protonation and/or deprotonation of COOH groups, may also contribute in this spectroscopic range. Above 1680  $\text{cm}^{-1}$ , signals from protonated heme propionates and, above 1710  $\text{cm}^{-1}$ , signals from protonated Asp and Glu are likely. In the spectrum in Figure 1 and the inset, signals at 1761 and 1751  $\text{cm}^{-1}$  and a broad band at 1736/1725  $\text{cm}^{-1}$  are observed in this region. After H–D exchange, characteristic shifts of the bands originating from protonated aspartates and glutamates of 4–10  $\text{cm}^{-1}$  can be observed in other systems (30, 31). In the spectrum of cytochrome *bd* shown in the inset of Figure 1, shifts of signals from 1734 to 1724  $\text{cm}^{-1}$  and from 1725 to 1716  $\text{cm}^{-1}$  can be seen. Hence, these signals can be tentatively assigned to the  $\nu(\text{C}=\text{O})$  mode of protonated aspartic and glutamic acids, coordinated by a relatively strong hydrogen bonding. Interestingly, the modes at 1761 and 1751  $\text{cm}^{-1}$  do not significantly shift upon H–D exchange. The efficiency of H–D exchange was found to exceed 70%, as determined by the decrease in the magnitude of the amide II mode at 1540  $\text{cm}^{-1}$  in FTIR absorbance spectra (data not shown). Possibly, the difference signals at 1761 and 1751  $\text{cm}^{-1}$  reflect the reorganization of protonated aspartic or glutamic acids which are not accessible to solvent. This possibility is supported by the positions of the modes, 1761 and 1751  $\text{cm}^{-1}$ , indicating weak hydrogen bonding of the COOH group, such as would be found for an acidic residue buried in a hydrophobic region of the protein. Alternatively, these bands might originate from the C=O group of the heme *d* chlorin ring. The  $\nu(\text{C}=\text{O})$  mode of isolated lactones is in this spectral range (32), but there is no supporting evidence from heme *d* model compounds for this assignment. Recently, Yamazaki et al. (25) presented FTIR difference spectra of photoreduced cytochrome *bd* from *E. coli* and observed similar spectroscopic features.

Signals originating from bound ubiquinone are expected in the frequency range from 1200 to 1700  $\text{cm}^{-1}$ . In the electrochemically induced FTIR difference spectrum of ubiquinone in aqueous solution, the split  $\nu(\text{C}=\text{O})$  modes of the oxidized quinone are at 1664 and 1652  $\text{cm}^{-1}$  and the  $\nu(\text{C}=\text{C})$  mode is at 1614  $\text{cm}^{-1}$ . At 1288 and 1268  $\text{cm}^{-1}$ , the signals from the C–OCH<sub>3</sub> vibrations of the 2- and 3-methoxy groups contribute (21, 24). The ring modes of the fully reduced and protonated forms of ubiquinol contribute to the

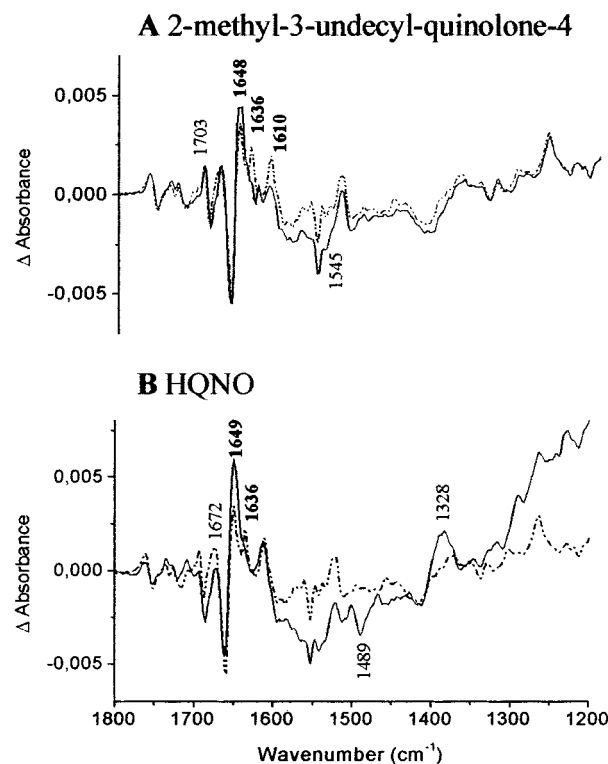


FIGURE 2: Oxidized-minus-reduced FTIR difference spectra of wild-type cytochrome *bd* from aerobically grown *E. coli* (···) in the presence of 2-methyl-3-undecylquinolone-4 [A (—)] as well as in the presence of HQNO [B (—)] for a potential step from −0.5 to 0.5 V (vs Ag/AgCl).

signals at 1494, 1470, 1424, and 1386  $\text{cm}^{-1}$ . The binding of the ubiquinone in the protein changes the vibrational modes of the quinone due to hydrogen bonding as well as changes in the orientation and configuration of the molecule bound to the protein. The  $\nu(\text{C}=\text{O})$  mode can be expected to shift to the region between 1670 and 1610  $\text{cm}^{-1}$  based on previous studies with other quinone-binding proteins. In the bacterial reaction center, for example, the  $\nu(\text{C}=\text{O})$  modes of Q<sub>A</sub> (22) and the  $\nu(\text{C}=\text{O})$  mode of the quinone bound to cytochrome *bo*<sub>3</sub> from *E. coli* (1652  $\text{cm}^{-1}$ ) (24) have been assigned to bands in this region. In the electrochemically induced FTIR difference spectrum of cytochrome *bd*, signals at 1649 and 1632  $\text{cm}^{-1}$  are observed in the spectral range for the C=O modes. In addition, a signal at 1616  $\text{cm}^{-1}$  can be tentatively assigned to the C=C mode. Modes involving the methoxy groups are likely to result in the signals at 1290 and 1263  $\text{cm}^{-1}$ . These two bands are very similar to those from quinone in solution, and they have been found to be largely insensitive toward the protein environment (21, 23, 24). The ring modes of the fully reduced and protonated forms of ubiquinol could be involved in the signals at 1494, 1474/1464, 1424, and 1385  $\text{cm}^{-1}$  on the basis of measurements of the spectra of model compounds (cf. Figure 3A, dotted line).

To support these tentative assignments, the effects of adding inhibitors directed at the quinone binding sites were studied in this work.

**Effect of Inhibitors.** Figure 2A shows the oxidized-minus-reduced FTIR difference spectra of cytochrome *bd* from *E. coli* for a potential step from −0.5 to 0.5 V in the presence (solid line) and absence (dashed and dotted line) of 2-methyl-3-undecylquinolone-4. 2-Methyl-3-undecylquinolone-4 is an

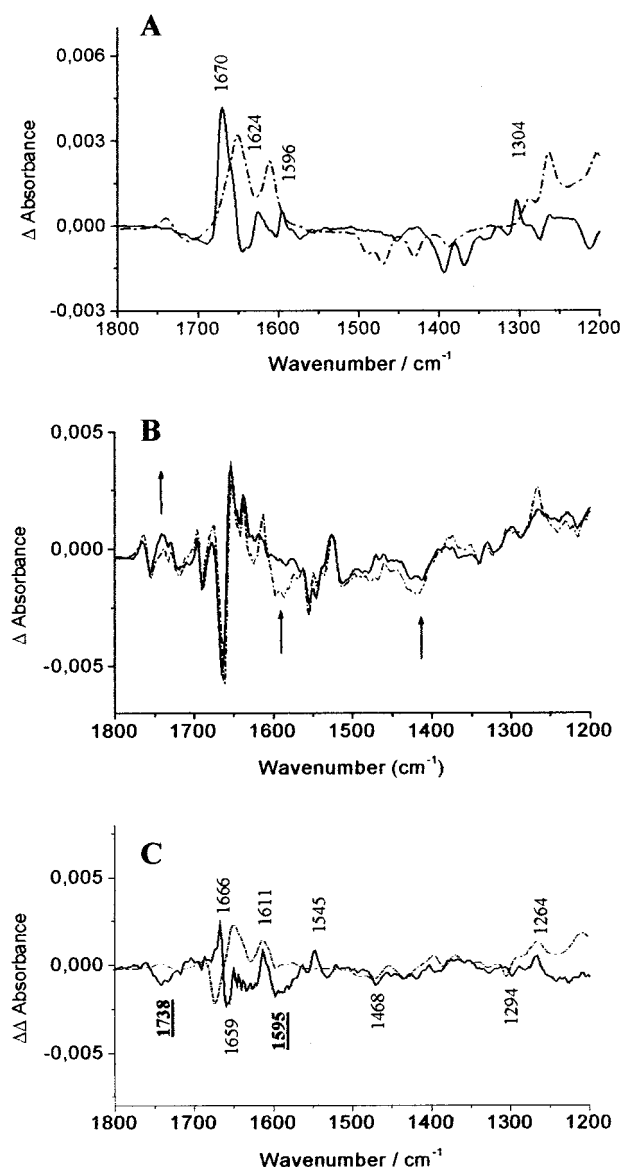


FIGURE 3: Oxidized-minus-reduced FTIR difference spectra of ubiquinone (---) and menaquinone (—) in aqueous solution (A) and of wild-type cytochrome *bd* from aerobically (---) and anaerobically (—) grown *E. coli* (B) and a double-difference spectrum calculated by subtraction of both spectra (—) and by subtraction of the spectra from ubiquinone and menaquinone (C).

inhibitor that is expected to act as the quinol binding site (38). It shows similarities to Aurachin D, which is a potent cytochrome *bd* inhibitor (33, 34), suggested to act at the quinol binding site and to affect heme *b*<sub>558</sub> as well as heme *b*<sub>595</sub> (16). It is noted that the addition of an inhibitor directed at the quinone binding site will not necessarily result in the complete displacement of the bound quinone in both the oxidized or reduced forms. This was recently shown for the *bc*<sub>1</sub> complex, where quinone was only partially displaced by potent inhibitors (40).

Clearly, variations occur in the electrochemically induced FTIR difference spectrum upon addition of 2-methyl-3-undecylquinolone-4. The decrease in the modes at 1636 and 1610 cm<sup>-1</sup> and the increase in the signal at 1648 cm<sup>-1</sup> can be seen. Further variations at approximately 1690 cm<sup>-1</sup> as well as in the broad modes at 1545 cm<sup>-1</sup> are observable. These effects can be attributed to the displacement or the partial displacement of the bound quinone by the binding of

2-methyl-3-undecylquinolone-4 and to concomitant changes in the protein such as the previously observed effect resulting from the binding of 2-methyl-3-undecylquinolone-4 on the visible spectrum of heme *b*<sub>558</sub> (16). As mentioned above, the  $\nu(\text{C}=\text{O})$  modes of ubiquinones in solution are observed as a broad and split mode at 1652 cm<sup>-1</sup>. The shift of these modes upon binding to the protein depends on the environment of the binding site. The signal which is observed to be shifted from 1636 to 1648 cm<sup>-1</sup> can be tentatively attributed to a  $\nu(\text{C}=\text{O})$  mode of the bound quinone which is displaced by 2-methyl-3-undecylquinolone-4. It is concluded that the displacement or partial displacement of the quinone by 2-methyl-3-undecylquinolone-4 changes the hydrogen bonding environment of one or both C=O groups. It may seem unusual that the inhibitor could be affecting only one of the C=O groups; however, on the other hand, this would be a likely explanation for partial quinone displacement as described before for the *bc*<sub>1</sub> complex, as mentioned above (40).

The variations from 1610 to 1620 cm<sup>-1</sup> occur in the spectral region characteristic for the  $\nu(\text{C}=\text{C})$  modes, and may reflect variations in the quinone ring as a result of its displacement by the inhibitor. Alternatively, the perturbation of the second C=O group may be observable in this region of the spectrum. If this is the case, the second C=O group of the bound quinone must be very strongly hydrogen bonded to the protein, meaning that the quinone would have an asymmetric orientation, as previously found for Q<sub>B</sub> in the bacterial reaction center (22). Finally, the decrease in the mode at 1680 cm<sup>-1</sup> together with the change at approximately 1545 cm<sup>-1</sup> could indicate the influence of the binding of 2-methyl-3-undecylquinolone-4 on the heme propionates of heme *b*<sub>558</sub>. Changes in secondary structure elements could also contribute in this spectral range, and isotope studies will be essential for definite assignments.

HQNO is another quinone analogue which is also a potent inhibitor of cytochrome *bd* from *E. coli*. Figure 2B shows the oxidized-minus-reduced FTIR difference spectra of cytochrome *bd* for a potential step from -0.5 to 0.5 V in the presence (solid line) and absence (dashed and dotted line) of HQNO. Consistent with the assignment based on the shift observed in the presence of 2-methyl-3-undecylquinolone-4, the mode at 1636 cm<sup>-1</sup> can be attributed to the  $\nu(\text{C}=\text{O})$  mode of the displaced quinone. Variations in the spectral range above 1690 cm<sup>-1</sup> indicate the perturbation of the  $\nu(\text{C}=\text{O})$  mode of protonated acidic residues, suggesting the involvement of COOH groups in quinone and/or HQNO binding. Unfortunately, the addition of HQNO induced some instability in the system, including the appearance of additional signals and baseline drift. Apparently, HQNO undergoes a redox reaction at the electrode, and the reaction products show redox-dependent contributions in FTIR. This was confirmed by the addition of excess HQNO and the concomitant increase in the modes at 1389 and 1489 cm<sup>-1</sup> (data not shown). Hence, apart from the shift of the band from 1636 to 1649 cm<sup>-1</sup>, additional reliable information was not obtained from the use of HQNO.

*Electrochemically Induced FTIR Difference Spectra of Cytochrome bd from Anaerobically Grown E. coli. (1) Spectra of Menaquinone and Ubiquinone in Aqueous Solution.* Figure 3A shows the oxidized-minus-reduced FTIR difference spectra of ubiquinone (dashed and dotted line) and

menaquinone (solid line) in solution. The FTIR bands from ubiquinone have been described above. In the FTIR redox difference spectrum of menaquinone, the split  $\nu(\text{C}=\text{O})$  mode is at  $1670\text{ cm}^{-1}$  with a shoulder at  $1658\text{ cm}^{-1}$ . The  $\nu(\text{C}=\text{C})$  mode of the quinoid ring is at  $1624\text{ cm}^{-1}$ , and that of the aromatic ring is at  $1596\text{ cm}^{-1}$ . The mode at  $1304\text{ cm}^{-1}$  has been previously attributed to a coupled  $\text{C}-\text{C}/\text{C}=\text{C}$  vibration (21).

(2) *Spectra of Menaquinone and Ubiquinones in the Protein Environment.* Panels A and B of Figure 3 show the oxidized-minus-reduced FTIR difference spectra of wild-type cytochrome *bd* from aerobically (dashed and dotted line) and anaerobically (solid line) grown *E. coli*. Also shown are double-difference spectra calculated by subtraction of the spectra shown in panels A and B of Figure 3 (solid line) and by subtraction of the spectra from ubiquinone and menaquinone in solution (dotted lines) (Figure 3C). The influence of the growth conditions on the quinone content and, thus, on the spectra of the purified protein is very substantial over the whole spectral range from  $1800$  to  $1200\text{ cm}^{-1}$ . When the growth conditions are switched from aerobic to anaerobic, the spectra show the decrease in band intensity attributed to bound ubiquinone and the increase in the menaquinone bands. For example, the mode at  $1264\text{ cm}^{-1}$ , attributed to the  $\text{C}-\text{O}$  vibration of the methoxy side chain (see above), is decreased and a small signal at  $1294\text{ cm}^{-1}$  appears in the enzyme from anaerobically grown cells (cf. Figure 3B). This mode is at a position close to the  $\text{C}-\text{C}/\text{C}=\text{C}$  mode observed for vitamin  $\text{K}_1$  at  $1304\text{ cm}^{-1}$  (Figure 3A) and is tentatively assigned to menaquinone bound to cytochrome *bd*. The shift of  $10\text{ cm}^{-1}$  is attributed to interactions between the protein site and the menaquinone ring. The fact that the band at  $1264\text{ cm}^{-1}$  is not completely abolished is due to residual ubiquinone bound to the enzyme, consistent with HPLC analysis (not shown). At  $1611\text{ cm}^{-1}$ , a band attributed to the  $\nu(\text{C}=\text{C})$  mode of ubiquinone increases in parallel with the ubiquinone content of the enzyme (Figure 3B,C). The  $\nu(\text{C}=\text{C})_{\text{aromatic}}$  mode of menaquinone is most likely responsible for part of the band at  $1595\text{ cm}^{-1}$  observed with the anaerobically grown enzyme. There are also changes observed in the spectral range of the  $\nu(\text{C}=\text{O})$  quinone modes, at  $1666$  and  $1659\text{ cm}^{-1}$ , but clear assignments are not possible without isotope labeling experiments. Notably, the signal at  $1635\text{ cm}^{-1}$  assigned to one of the carbonyl groups of bound ubiquinone (see above) does not change upon replacement of ubiquinone by menaquinone, indicating similar environments for one of the  $\text{C}=\text{O}$  groups in both cases. Changes between  $1560$  and  $1530\text{ cm}^{-1}$  may include modes that reflect changes in heme vibrations as well as secondary structure elements.

The most interesting spectroscopic difference between the cytochrome *bd* from anaerobic and aerobic growth conditions is observed at  $1738\text{ cm}^{-1}$ , in the spectral range where the contribution of protonated aspartic and glutamic acids can be expected. Clearly, the difference signal is increased in the spectrum of the enzyme from anaerobically grown *E. coli*. Deprotonated acidic residues contribute at  $\sim 1590\text{ cm}^{-1}$ , and indeed, there is a distinct decrease in a mode at  $1595\text{ cm}^{-1}$  compared to what is observed in the difference spectrum of cytochrome *bd* isolated from the aerobic cells. The data are consistent with a change in the protonation state of a glutamic or aspartic acid group depending on whether

ubiquinone (deprotonated) or menaquinone (protonated) is bound to cytochrome *bd*.

## CONCLUSIONS

Cytochrome *bd* from *E. coli* can utilize either ubiquinol or menaquinol as a substrate. The current work provides direct, spectroscopic evidence for the first time that the protein can bind to either substrate. It is also shown that the binding of the inhibitor 2-methyl-3-undecylquinolone-4 or HQNO results in the apparent displacement of bound ubiquinone, as evidenced from the perturbation of the FTIR spectrum of the protein-bound quinone.

The data also provide evidence for the differences in the interactions of cytochrome *bd* from *E. coli* with ubiquinone and ubiquinol, and menaquinone and menaquinol. Furthermore, the data explicitly point to a role of acidic residues in the binding interactions of the respective quinones. Changes in the FTIR difference spectra show perturbations from protonated carboxyl groups upon oxidation–reduction changes of the enzyme, extending previously published work (25). Although speculative, the data suggest the possible influence of a heme center in the protein response to quinone redox changes, as reflected by changes at  $1595\text{ cm}^{-1}$  as well as at  $1561$ – $1545\text{ cm}^{-1}$ . This is in line with a previous work by J  nemman et al. (16) indicating that the quinone/inhibitor binding site(s) is close to the hemes *b*.

It is noted that aspartic and glutamic acids are common hydrogen bonding partners for the protein-bound quinones, including stabilization of the radical semiquinone. Acidic residues have also been implicated in proton uptake or release accompanying quinone reduction or oxidation, respectively (for example, in refs 35–37). Indeed, the spectroscopic changes observed in the current work indicate that an aspartic or glutamic acid residue is protonated in the oxidized state of the enzyme in the anaerobically grown samples, i.e., when the enzyme is bound to menaquinone. When ubiquinone is bound to the oxidized form of the enzyme, an aspartate or glutamate residue appears to be deprotonated. Most likely, one amino acid residue is responsible for these experimental observations, thus indicating that the protonation change of an acidic residue is part of the adaptation of the quinone binding site that allows the binding and effective electron transfer from the different quinone types. The significance of this observation will require further work. Site-directed mutagenesis might be useful in this regard. Sequence alignments have shown two highly conserved glutamic acid residues (E99 and E107) in transmembrane helix III of subunit I and another (E257) within the hydrophilic Q loop (12). Possibly, one of these residues is directly involved in quinone or quinol binding.

## ACKNOWLEDGMENT

We are grateful to Prof. Dr. W. M  ntele for kindly providing the electrochemical cell.

## SUPPORTING INFORMATION AVAILABLE

HPLC detection and quantification of quinone bound to membrane and cytochrome *bd* purified from anaerobically and aerobically grown *E. coli*. One ubiquinone and one menaquinone, in a 1:1 ratio, have been determined per purified cytochrome *bd* grown anaerobically, and 0.5 ubiquino-

ne per purified cytochrome *bd* grown aerobically. We note that this value depends on the efficiency of the quinone extraction, and the amount of quinone bound to the purified protein itself is highly dependent on the preparation. This material is available free of charge via the Internet at <http://pubs.acs.org>.

## REFERENCES

1. Kita, D., Konishi, K., and Anraku, Y. (1984) *J. Biol. Chem.* 259, 3375–3381.
2. Anraku, Y., and Gennis, R. B. (1987) *Trends Biochem. Sci.* 12, 262–266.
3. Rice, C. W., and Hempfling, W. P. (1978) *J. Bacteriol.* 134, 115–124.
4. Fu, H.-A., Iuchi, S., and Lin, E. C. C. (1991) *Mol. Gen. Genet.* 226, 209–213.
5. Cotter, P. A., Chepuri, V., Gennis, R. B., and Gunsalus, R. P. (1990) *J. Bacteriol.* 172, 6333–6338.
6. Mogi, T., Tsubaki, M., Hori, H., Miyoshi, H., Nakamura, H., and Anraku, Y. (1998) *J. Biochem., Mol. Biol. Biophys.* 2, 79–110.
7. Hill, J. J., Alben, J. O., and Gennis, R. B. (1993) *Proc. Natl. Acad. Sci. U.S.A.* 90, 5863–5867.
8. Jasaitis, A., Borisov, V. B., Belevich, N. P., Morgan, J. E., Konstantinov, A. A., and Verkhovsky, M. I. (2000) *Biochemistry* 39, 13800–13809.
9. Yang, F. D., Yu, L., Yu, C. A., Lorence, R. M., and Gennis, R. B. (1986) *J. Biol. Chem.* 261, 14987–14990.
10. Lorence, R. M., Carter, K., Gennis, R. B., Matsushita, K., and Kaback, H. R. (1988) *J. Biol. Chem.* 263, 5271–5276.
11. Dueweke, T. J., and Gennis, R. B. (1991) *Biochemistry* 30, 3401–3406.
12. Osborne, J. P., and Gennis, R. B. (1999) *Biochim. Biophys. Acta* 1410, 32–50.
13. Hastings, S. F., and Ingledew, W. J. (1996) *Biochem. Soc. Trans.* 24, 131–132.
14. Hastings, S. F., Kaysser, T. M., Jiang, F., Salerno, J. C., Gennis, R. B., and Ingledew, W. J. (1998) *Eur. J. Biochem.* 225, 317–323.
15. Meunier, B., Madgwick, S. A., Reil, E., Oettmeier, W., and Rich, P. R. (1995) *Biochemistry* 34, 1076–1083.
16. Jünemann, S., Wrigglesworth, J. M., and Rich, P. R. (1997) *Biochemistry* 36, 9323–9331.
17. Wallace, B. J., and Young, I. G. (1977) *Biochim. Biophys. Acta* 461, 75–83.
18. Hollander, R. (1976) *FEBS Lett.* 72, 98–100.
19. Prince, R. C., Dutton, P. L., and Bruce, J. M. (1983) *FEBS Lett.* 160, 273–276.
20. Hastings, S., Heathcote, P., Ingledew, W. J., and Rigby, S. E. J. (2000) *Eur. J. Biochem.* 267, 5638–5645.
21. Breton, J., Burie, J. R., Berthomieu, C., Berger, G., and Navedryk, E. (1994) *Biochemistry* 33, 4953–4965.
22. Breton, J., Boullais, C., Burie, J. R., Navedryk, E., and Mioskowski, C. (1994) *Biochemistry* 33, 14378–14386.
23. Bayman, F., Robertson, D. E., Dutton, P. L., and Mäntele, W. (1999) *Biochemistry* 38, 13188–13199.
24. Hellwig, P., Mogi, T., Tomson, F. L., Gennis, R. B., Iwata, J., Miyoshi, H., and Mäntele, W. (1999) *Biochemistry* 38, 14683–14689.
25. Yamazaki, Y., Kandori, H., and Mogi, T. (1999) *J. Biochem.* 125, 1131–1136.
26. Zhang, J., Hellwig, P., Osborne, J. P., Huang, H. W., Moenne-Loccoz, P., Konstantinov, A. A., and Gennis, R. B. (2001) *Biochemistry* 40, 8548–8556.
27. Moss, D., Navedryk, E., Breton, J., and Mäntele, W. (1990) *Eur. J. Biochem.* 187, 565–572.
28. Mäntele, W. (1993) *Trends Biochem. Sci.* 18, 197–202.
29. Hellwig, P., Behr, J., Ostermeier, C., Richter, O.-M. H., Pfitzner, U., Odenwald, A., Ludwig, B., Michel, H., and Mäntele, W. (1998) *Biochemistry* 37, 7390–7399.
30. Siebert, F., Mäntele, W., and Kreutz, W. (1982) *FEBS Lett.* 141, 82–87.
31. Pinchas, S., and Laulicht, I. (1977) *Infrared Spectra of Labelled Compounds*, Academic Press, London.
32. Herzberg, G. (1962) in *Molecular spectra and molecular structure: II. Infrared and Raman spectra of polyatomic molecules*, D. Van Nostrand Co., Princeton, NJ.
33. Oettmeier, W., Masson, K., Soll, M., and Reil, E. (1994) *Biochem. Soc. Trans.* 22, 213–216.
34. Reil, E., Soll, M., Masson, K., and Oettmeier, W. (1994) *Biochem. Soc. Trans.* 22 (1), 62.
35. Crofts, A. R., Hong, S., Ugulava, N., Barquera, B., Gennis, R. B., Guergova-Kuras, M., and Berry, E. A. (1999) *Proc. Natl. Acad. Sci. U.S.A.* 96, 10021–10026.
36. Hellwig, P., Barquera, B., and Gennis, R. B. (2001) *Biochemistry* 40, 1077–1082.
37. Okamura, M. Y., Paddock, M. L., Graige, M. S., and Feher, G. (2000) *Biochim. Biophys. Acta* 1458, 148–163.
38. Reil, E., Höfle, G., Draber, W., and Oettmeier, W. (1997) *Biochim. Biophys. Acta* 1318, 291.
39. Miller, M. J., and Gennis, R. B. (1983) *J. Biol. Chem.* 258, 9159–9165.
40. Bartoschek, S., Johansson, M., Geierstanger, B. H., Okun, J. G., Lancaster, C. R., Humpfer, E., Yu, L., Yu, C. A., Griesinger, C., and Brandt, U. (2001) *J. Biol. Chem.* 38, 35231–35234.

BI011784B